

# A classical field theory formulation for the numerical solution of time harmonic electromagnetic fields

A. Gold\*

Stanford University, Stanford, California 94305, USA

S. Tantawi

SLAC National Accelerator Laboratory, Menlo Park, California 94025, USA

(Dated: September 4, 2022)

Finite element representations of Maxwell’s equations pose unusual challenges inherent to the variational representation of the “curl-curl” equation for the fields. We present a variational formulation based on classical field theory. Borrowing from QED, we modify the Lagrangian by adding an implicit gauge-fixing term. Our formulation, in the language of differential geometry, shows that conventional edge elements should be replaced by the simpler nodal elements for time-harmonic problems. We demonstrate how this formulation, adhering to the deeper underlying symmetries of the four-dimensional covariant field description, provides a highly general, robust numerical framework.

As physicists and engineers seek to model increasingly complex electromagnetic systems, from radio-frequency power sources to integrated photonics, the need for efficient and robust full-wave first principles numerical fields solvers is growing. Finite element (FE) methods, which solve partial differential equations over a discretized problem domain (often a spatial mesh), are a natural solution enjoying widespread use in fields from fluid dynamics to structural mechanics.

Unfortunately, in electromagnetic problems, the variational formulation driving the FE method presents unique challenges which impede the computational efficiency and accuracy of existing solvers. For time harmonic problems, the focus of this paper, this variational expression is given by eq. 1. For a more detailed treatment and a definition of terms see for example [1].

$$F[\vec{E}] = \int \frac{1}{2\mu_r} (\nabla \times \vec{E})^2 - \frac{k_0^2 \epsilon_r}{2} \vec{E}^2 + \vec{E} \cdot \vec{J} dV \quad (1)$$

The challenge consists in enforcing the divergence constraint associated with Gauss’s law,  $\nabla \cdot \vec{E} = 0$  or the Coulomb gauge,  $\nabla \cdot \vec{A} = 0$  while ensuring adequate freedom in the basis functions (functions used to expand the approximate solution in each mesh element) to model discontinuities in the fields [2, 3]. These two requirements conflict in standard nodal element based finite element (FE) methods, employed successfully in other fields such as fluid mechanics and structural mechanics.

Additionally, eq. 1 does not provide the flexibility to drive the fields with space charge density,  $\rho$ , but only accounts for contributions from the current density,  $\vec{J}$ . This is a significant shortcoming in modeling for example beam driven radiation sources or low frequency electro-quasi statics where the space charge driven fields are non-negligible.

To resolve these issues, we propose a formulation for the finite element solution of electromagnetic systems based on the classical field theory Lagrangian with a

gauge fixing term adapted from quantum electrodynamics. This is given in the framework of differential geometry by eq. 2, where we adopt the standard terminology given by introductory texts such as [4]. As will be introduced in greater detail shortly, the first two terms constitute the classical Lagrangian and the final term, multiplied by the scalar  $\frac{1}{2\xi}$ , is the gauge fixing addition.

$$\mathcal{L} = -\frac{1}{2} d\mathbf{A} \wedge \star d\mathbf{A} + \mathbf{A} \wedge \mathbf{J} - \frac{1}{2\xi} d \star \mathbf{A} \wedge \star d \star \mathbf{A} \quad (2)$$

Here  $\mathbf{A} = A_\mu dx^\mu$  is the four dimensional (4D) differential 1-form,  $A_\mu = (\frac{\phi}{c}, \vec{A})$  is the four-potential, and  $\mathbf{J}$  is the current 3-form. Instead of taking the variation of eq. 1 to obtain  $\vec{E}$ , we propose taking the variation of  $F[\mathbf{A}] = \int \mathcal{L} dx^4$ . This formulation fully accounts for the charge density,  $\rho$  as  $J_\mu = (c\rho, \vec{J})$  and, as we will elaborate on later, facilitates a return to the widely used nodal FE framework.

We motivate this idea by considering how the challenges inherent to eq. 1 are currently resolved. Enforcing the divergence constraint was initially addressed by adding a regularization term of the form  $s(\nabla \cdot \vec{E})^2$  to eq. 1, with limited success[5, 6]. In fact, it was only recently that this regularization was proven to overly restrict the solution space when applied in nodal element formulations. When singularities in the field exist such as sharp corners, the missing subspace not spanned by the nodal elements consists of the gradients of solutions to Laplace’s equation [7–9]. One can thus supplement the nodal basis functions with additional singular or non-conforming functions [10–12], or relax the regularization term near the singularity [13–15]. The former requires computing the coupling between the nodal basis and the singular functions and is challenging to extend to three dimensions while latter is a compromise between enforcing the divergence constraint over the problem domain and not completely restricting the subspace spanned by gradients.

A more robust solution arises when viewing electromagnetism through the lens of differential geometry. In 3D Euclidean space, the edge elements are the natural discrete basis for  $\vec{E}$  (and  $\vec{A}$  in the Coulomb gauge), both differential 1-forms. By their construction, only tangential continuity is imposed at the faces between elements, resolving the issue of modeling field discontinuities at interfaces and boundaries. However, while the edge elements are divergence-free locally, the discontinuity in the normal field at element interfaces allows for solutions that are not divergence-free globally. The space spanned by edge elements divides into the desired space of weakly divergence-free fields and its co-domain, the kernel of the curl operator (purely gradient functions in topologically trivial domains) [16]. There are methods to extract the gradient field so as to span only the divergence-free fields, such as the tree-cotree method [17–20]. However, choosing an optimal tree is challenging and poor conditioning of the final linear system is a common issue [21–24].

Interestingly, to the author’s knowledge, efforts at employing differential geometry to numerical electromagnetism are constrained to 3D Euclidean space. Meanwhile, electromagnetic theory is encoded much more succinctly by differential geometry in 4D Minkowski space, where deeper underlying structure is made explicit, such as gauge and Lorenz invariance. For Lorenzian manifolds, the equations for the field are given by eqs. 3-4 where  $\mathbf{F} = d\mathbf{A}$  is the electromagnetic field tensor and  $\mathbf{J}$  is the current 3-form defined earlier.

$$d\mathbf{F} = 0 \quad (3) \quad d\star\mathbf{F} = \mathbf{J} \quad (4)$$

The classical field theory Lagrangian can be written in terms of  $\mathbf{A}$  as:

$$\mathcal{L} = -\frac{1}{2}d\mathbf{A} \wedge \star d\mathbf{A} + \mathbf{A} \wedge \mathbf{J} \quad (5)$$

It is clearly more natural to work with  $\mathbf{A}$  than  $\mathbf{E}$  and  $\mathbf{B}$ , the 3D components of the two-form  $\mathbf{F}$ , with the additional benefit that eq. 3 is automatically satisfied as  $d^2 = 0$ . As in 3D Euclidean space, where there is a duality between 1-forms and edges, in a 4D mesh the 1-form  $\mathbf{A}$  should be expanded using edge elements. This is an interesting idea to pursue for transient numerical analysis, however in the case of time harmonic problems we head in a different direction. The time dimension of the mesh is collapsed and edges of the 4D mesh become points in a 3D mesh. As such, *nodal* elements should be employed to expand  $\mathbf{A}$  rather than the more complicated edge elements.

The resulting linear system from employing eq. 5 in the finite element method is, unfortunately, highly ill-conditioned. This comes as no surprise when considering that unlike the fields, the four potential is not uniquely defined. The Lagrangian is invariant to gauge transformations of the form  $\mathbf{A} \rightarrow \mathbf{A} + d\psi$  where  $\psi$  is a scalar 0-form. To resolve this issue, we applied a solution to a

similar challenge in quantum electrodynamics (QED). In the field discretization, the resulting (symbolic) matrices are singular due to gauge invariance, which is resolved by adding a gauge fixing term to the Lagrangian [25]:

$$\mathcal{L}_{\text{GF}} = -\frac{1}{2\xi}d\star\mathbf{A} \wedge \star d\star\mathbf{A} \quad (6)$$

In QED, the gauge fixing term imposes different gauges depending on the value of  $\xi$ . In our classical context, any  $\xi \neq 0$  imposes the Lorenz gauge with residual gauge freedom  $\psi|\nabla^2\psi - k_0^2\psi = 0$ . By setting  $\mathbf{A}$  explicitly on the boundary,  $\psi$  is forced to zero on the boundary, and hence everywhere, and  $\mathbf{A}$  will be unique.

Tempting as this may be, doing so in the most straightforward way (setting  $\vec{A}_t = 0$  and  $\phi = 0$  on the boundary for a perfect electric conductor, or  $\vec{A}_n = 0$  and  $\nabla_n\phi = 0$  for a perfect magnetic conductor) in fact decouples  $\phi$  from  $\vec{A}$ . This reduces the problem to two separate wave equations, eq. 7 amenable to nodal elements and eq. 8 which reduces to the curl-curl equation for  $\vec{A}$  and must be solved via edge elements.

$$\nabla^2\phi - \frac{1}{c^2}\frac{\partial^2\phi}{\partial t^2} = -\frac{\rho}{\epsilon} \quad (7)$$

$$\nabla^2\vec{A} - \frac{1}{c^2}\frac{\partial^2\vec{A}}{\partial t^2} = -\mu\mathbf{j} \quad (8)$$

This decoupled, mixed formulation approach has been adopted by some low-frequency eddy current solvers. While some suggest they are using a Lorenz gauge condition, in these implementations the Lorenz gauge simplifies to the usual divergence free condition on  $\vec{A}$  and the two components are coupled only in the sense that their excitations are related through the charge continuity equation,  $\nabla \cdot \vec{J} = i\omega\rho$  [26].

Instead, we allow the residual gauge freedom to persist by imposing boundary conditions solely through surface integrals, as would be necessary anyway for impedance or absorbing boundary conditions. In contrast to the mixed formulations, the resulting solution is not a simple superposition of independent solutions for  $\vec{A}$  and  $\phi$ , but a self-consistent solution for  $\mathbf{A}$  in its entirety. This, in conjunction with the gauge fixing term, is what enables the use of nodal elements in the four-potential formulation compared to existing  $\vec{A} - \phi$  formulations [19, 26–29].

With regards to computational implementation, some new challenges arise with our formulation. Firstly, for eigenmode analysis (the focus of this paper), the coupling between  $\vec{A}$  and  $\phi$  results in a quadratic eigenvalue problem instead of the regular eigenvalue problem of the curl-curl equation. In our proof of concept implementation we use the sparse non-linear eigenvalue solver, NLFEST [30]. Given the singular nature of the resulting finite element system, an alternative and possibly preferable choice might be a singular value decomposition (SVD) solver. Despite being singular, however, the condition

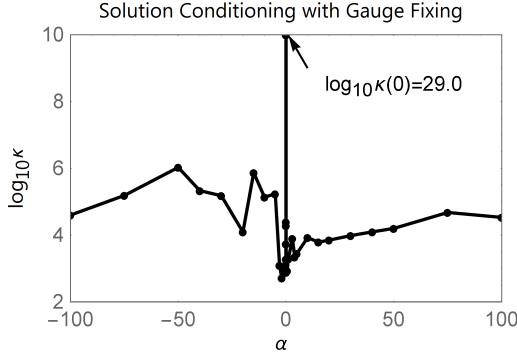


FIG. 1: Condition number,  $\kappa$ , as a function of gauge fixing term  $\alpha$  for the eigenvalue corresponding to the fundamental mode of the cavity shown in fig. 5.

number of the eigenvalues, as defined in [31], are reasonable and uncorrelated to problem size. The conditioning does depend on the gauge fixing term, as shown for a typical problem in fig 1. The need for this term is evident from the singularity at  $\alpha = \frac{1}{2\xi} = 0$ .

Secondly, the natural boundary condition corresponds to a perfect magnetic boundary. Imposing a perfect conducting boundary requires adding an appropriate surface term similar to an impedance, absorbing or radiative boundary condition. We implemented the surface term in eq. 9 for the perfect electric boundary, setting  $\gamma$  to a large number to force  $E_t \rightarrow 0$ .

$$S_{PE} = \gamma \int_{\partial\Omega} \left| \left( -\nabla\phi - i\omega\vec{A} \right) \times \hat{n} \right|^2 dS \quad (9)$$

We now present benchmarking results, computing the eigenmodes of some sample problems. In the eigenmode analysis, there are no source terms, and one seeks to compute the eigenvalues ( $k_0$ ) and eigenvectors ( $\mathbf{A}$ ). This is in contrast to driven solutions, where the frequency is known a-priori from the source terms. The examples shown are axisymmetric, solved in a cylindrical coordinate system:  $(r, \theta, z)$  on a 2D mesh with  $r, z$  in-plane and  $\theta$  out of plane. All figures plotting mode profiles are cross sectional views of the  $(z, r)$  plane (ie. the x axis is the axis of revolution), and the example cavities are 1m by 1m. The fields split into modes which can be represented by  $A_\theta$  alone (transverse electric), or as a combination of  $A_z, A_r$ , and  $\phi$  (transverse magnetic). The former are not susceptible to the challenges discussed previously so we focus on the in-plane components.

For comparison, we used COMSOL, a commercially available edge-element solver. It is capable of solving axisymmetric in-plane fields on a 2D mesh, allowing for a comparison with our computational implementation in terms of accuracy and problem size. We refer the reader to [32] for exact implementation details.

The cylindrical pillbox cavity is a good initial test case as the analytical solution exists. Figure 2 shows the cross

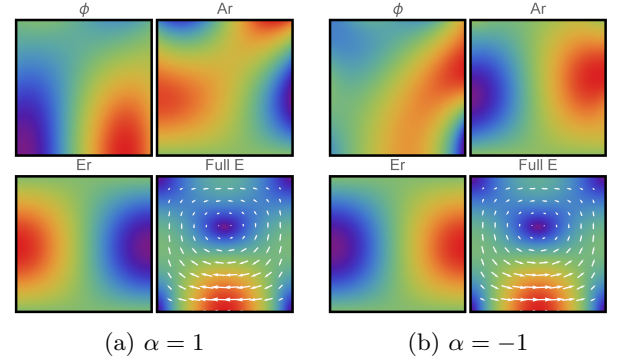


FIG. 2: FE solution for the fundamental mode of a pillbox cavity with perfect magnetic boundary. We plot two distinct solutions for  $\mathbf{A}$  (computed with different  $\alpha$ ), however the computed fields are the same.

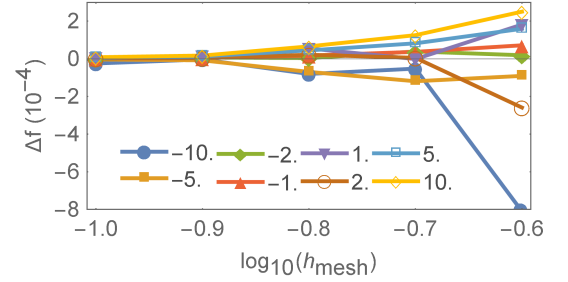


FIG. 3: Error in the frequency,  $\Delta f = \frac{f_{FE} - f_{theor}}{f_{theor}}$  for various values of  $\alpha$ . The variation in solved frequency decreases as the mesh is refined.

sectional problem geometry and the mode profiles for  $\phi, A_r$  and  $A_z$  for two different values of the gauge fixing term. Changing  $\alpha$  numerically perturbs the system, producing a solution with a different residual gauge,  $\psi$ . Nonetheless, the resonant frequencies and fields calculated from the different solutions for the four-potential correspond to the same, correct mode. An interesting consequence of calculating different  $\mathbf{A}$  for the same mode is that the numerical error is different in each case, as demonstrated by fig. 3. As the mesh is refined, all solutions converge to the same frequency. Plotting this convergence, now for only a few values of  $\alpha$ , fig. 4 demonstrates similar convergence characteristics for both the nodal and edge elements, matching that predicted from theory for second order elements.

Moving on to problems where nodal elements fail, fig. 5 plots the solution for a notched pillbox cavity with a field singularity on the corner and a perfect electric boundary. The discontinuity in the fields at the notch is fully captured in  $\nabla\phi$  while the four-potential is continuous.

In fig. 6, the solution error is plotted as a function of the number of degrees of freedom solved for. The absolute accuracy relative to problem size is comparable despite the additional degree of freedom used in the four-

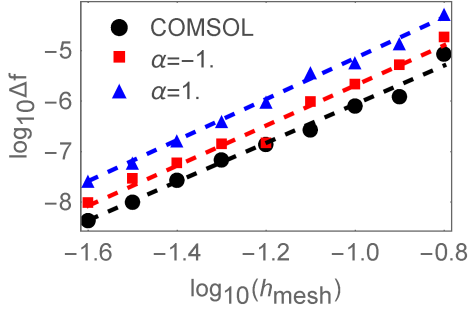


FIG. 4: Convergence of the frequency for the mode in fig. 2 with mesh size,  $h_{mesh}$ . The slopes of the linear fits are 3.83 (COMSOL), 3.97 ( $\alpha = -1$ ) and 4.06 ( $\alpha = 1$ ), agreeing with the expected convergence,  $O(h^4)$ .

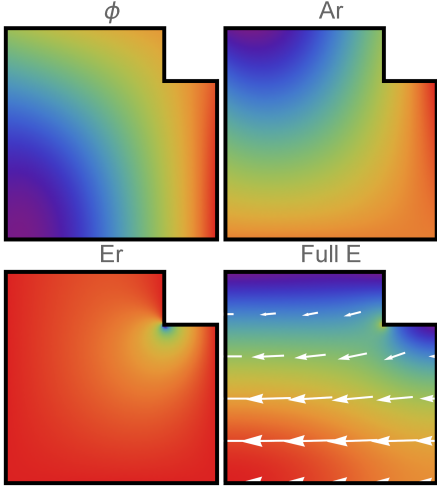


FIG. 5: FE solution for the fundamental mode of a notched pillbox cavity.  $\phi$ ,  $A_r$  are continuous but the singularity is captured in the computed fields.

potential formulation, a result that is consistent over all problems we considered. This is not surprising: edge element result in roughly twice as many degrees of freedom as nodal elements due to the additional degrees of freedom per mesh triangle and the fact that there are many more edges than nodes in a mesh[1, 34].

In addition to field singularities, the four-potential formulation can model discontinuities at material interfaces without the special treatment typically required to accommodate the jump in the normal field[1]. Figure 7 shows the field profile for a tapered dielectric lined cavity.  $\phi$  and  $\vec{A}$  are continuous but  $\nabla\phi$  captures the discontinuity in the fields due to the change in  $\epsilon_r$ .

Concluding, we have demonstrated a new finite element formulation to solve time harmonic electromagnetic fields. By encoding the physics of electromagnetism in a different mathematical formulation, the Lagrangian formulation does not suffer from the challenges inherent to the conventional curl-curl equation for  $\vec{E}$ . In contrast to

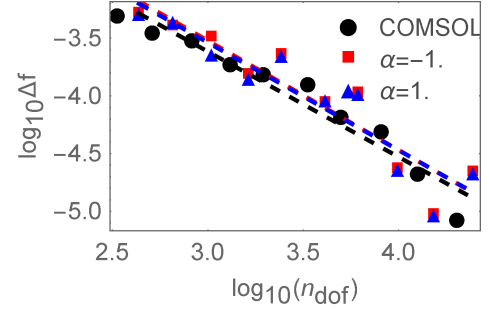


FIG. 6: Convergence of the frequency,  $f_0$ , for the mode in fig. 5 with problem size,  $n_{DOF}$ , for two different residual gauges, set by varying  $\alpha = 1/2\xi$ .

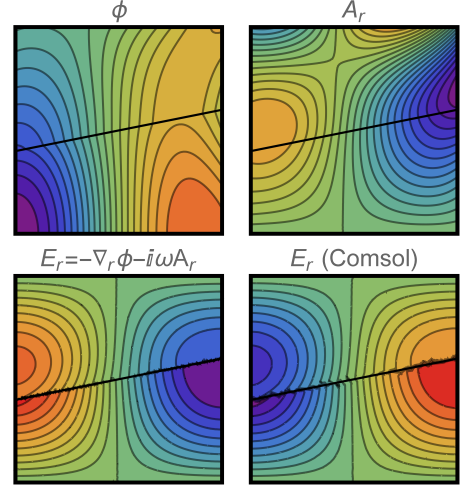


FIG. 7: FE solution for the fundamental mode of a dielectric lined cavity with  $\epsilon_r = 1.5$  above the thick back line. The resonant frequency is  $f_0 = 214.051$  MHz compared to 214.054 MHz in COMSOL.

the curl-curl equation, where  $\vec{J}$  is the only driving term, our formulation completely accounts for both  $\vec{J}$  and  $\rho$  in the source terms. The residual gauge freedom provides the flexibility for fields to be driven by both, a feature not relevant in the eigenmode analysis but which we can show for driven problems. This is of importance in the analysis of beam driven radiation sources for example.

Finally, we show through both theory and experimental results that the nodal elements are the correct basis choice for our 4D formulation. Indeed, our implementation demonstrates that the four-potential formulation easily handles field singularities and discontinuities unlike nodal element curl-curl implementations. This is not only beneficial in terms of the computational efficiency and simplicity of nodal elements, but given the widespread use of nodal elements in fields from structural mechanics to fluid dynamics, it allows for a common framework for multi-physics problems.

This project was funded by U.S. Department of Energy

under Contract No. DE-AC02-76SF00515.

---

\* vrielink@stanford.edu

- [1] J. Jin, *The Finite Element Method in Electromagnetics*, Wiley - IEEE (Wiley, 2015).
- [2] R. Albanese and G. Rubinacci (Elsevier, 1997) pp. 1 – 86.
- [3] I. Cortes Garcia, S. Schöps, H. De Gersem, and S. Baumanns, arXiv e-prints , arXiv:1802.06673 (2018), arXiv:1802.06673 [math.NA].
- [4] J. Stoker, *Differential Geometry*, Pure and applied mathematics (Wiley, 1989).
- [5] L. Demkowicz, “Finite element methods for maxwell’s equations,” in *Encyclopedia of Computational Mechanics Second Edition* (American Cancer Society, 2017) pp. 1–20.
- [6] S. Adam, P. Arbenz, and R. Geus, Technische Berichte/ETH Zürich, Departement Informatik **275** (1997).
- [7] M. Costabel and M. Dauge (Springer, 2003) pp. 125–161.
- [8] M. Costabel and M. Dauge, *Archive for Rational Mechanics and Analysis* **151**, 221 (2000).
- [9] F. Assous, P. Ciarlet Jr., P.-A. Raviart, and E. Sonnendrücker, *Mathematical Methods in the Applied Sciences* **22**, 485 (1999).
- [10] A. Dhia, C. Hazard, and S. Lohrengel, *SIAM Journal on Applied Mathematics* **59**, 2028 (1999).
- [11] F. Assous, P. Ciarlet, and E. Sonnendrücker, *Modélisation Mathématique et Analyse Numérique* **32**, 359 (1998).
- [12] H.-Y. Duan, R. C. Tan, S.-Y. Yang, and C.-S. You, *Journal of Computational Physics* **268**, 63 (2014).
- [13] M. Costabel and M. Dauge, *Numerische Mathematik* **93**, 239 (2002).
- [14] Ciarlet Jr., Patrick, Lefèvre, François, Lohrengel, Stéphanie, and Nicaise, Serge, *ESAIM: M2AN* **44**, 75 (2010).
- [15] R. Otin, *Electromagnetics* **30**, 190 (2010).
- [16] A. Bossavit and I. Mayergoyz, *Computational Electromagnetism: Variational Formulations, Complementarity, Edge Elements*, Electromagnetism (Elsevier Science, 1998).
- [17] R. Albanese and G. Rubinacci, *IEEE Transactions on Magnetics* **24**, 98 (1988).
- [18] B. Trapp, H. Munteanu, R. Schuhmann, T. Weiland, and D. Ioan, *IEEE Transactions on Magnetics* **38**, 445 (2002).
- [19] R. Wang, D. J. Riley, and J. Jin, *IEEE Transactions on Antennas and Propagation* **58**, 1590 (2010).
- [20] J. Manges and Z. Cendes, *International Journal for Numerical Methods in Engineering* **40**, 1667 (1997).
- [21] I. Ticar, O. Biro, and K. Preis, *IEEE Transactions on Magnetics* **38**, 437 (2002).
- [22] N. A. Golias and T. D. Tsiboukis, *IEEE Transactions on Magnetics* **30**, 2877 (1994).
- [23] K. Preis, I. Bardi, O. Biro, C. Magele, G. Vrisk, and K. R. Richter, *IEEE Transactions on Magnetics* **28**, 1056 (1992).
- [24] A. Ahagon and A. Kameari, *IEEE Transactions on Magnetics* **53**, 1 (2017).
- [25] M. Schwartz, *Quantum Field Theory and the Standard Model*, Quantum Field Theory and the Standard Model (Cambridge University Press, 2014) Chap. 8.5.1.
- [26] Y. Li, S. Sun, Q. I. Dai, and W. C. Chew, *IEEE Transactions on Antennas and Propagation* **64**, 4355 (2016).
- [27] H. Duan, R. Tan, S. Yang, and C. You, *SIAM Journal on Scientific Computing* **40**, A224 (2018).
- [28] S. Baumanns, M. Clemens, and S. Schps, in *2013 International Symposium on Electromagnetic Theory* (2013) pp. 1007–1010.
- [29] C. Amrouche, C. Bernardi, M. Dauge, and V. Girault, *Mathematical Methods in the Applied Sciences* **21**, 823 (1998).
- [30] B. Gavin, A. Midlar, and E. Polizzi, *Journal of Computational Science* **27**, 107 (2018).
- [31] F. Tisseur and K. Meerbergen, *SIAM Rev.* **43**, 235 (2001).
- [32] *COMSOL Multiphysics Reference Manual*.
- [33] A. Kameari, *IEEE Transactions on Magnetics* **35**, 1394 (1999).
- [34] G. Mur, *IEEE Transactions on Magnetics* **30**, 3552 (1994).